

# Antiproton physics with PANDA at FAIR

E. Tomasi-Gustafsson\*

*CEA, IRFU, SPhN, 91191 Gif-sur-Yvette Cedex, France*

*and*

*CNRS/IN2P3, Institut de Physique Nucléaire, UMR 8608, 91406 Orsay, France*

## Abstract

A high intensity antiproton beam of momentum up to 15 GeV/c will be available at FAIR in next future. The PANDA experiment, which is integrated in the storage ring for antiprotons, is at the center of the hadron physics program at this facility. It includes among other topics like hadron spectroscopy in the charmonium mass region, hyperon physics and electromagnetic processes. This contribution describes the facility, the detector and the relevant physics issues, with special focus on electromagnetic proton form factors in the time-like region.

## 1 Introduction

An international facility, FAIR (Facility for Antiproton and Ion Research) is under construction in Europe, gathering more than 3000 scientists from 50 countries, to study fundamental problems in physics research and applications [1]. The new facility is built at Darmstadt, at the site of GSI, and will make use and extend the existing structure and accelerators which will serve as a pre-accelerators.

Different beams of unprecedented quality will be accelerated and delivered to the different areas, allowing to carry out different programs in parallel. In the final construction FAIR will consist of eight ring with up to 1,100 m in circumference, two linear accelerators and about 3.5 km of beam control tubes.

High intensity beams from proton (of intensity up to  $3 \times 10^{13}$  and energy up to 30 GeV) to uranium will be used directly for different physics programs and to produce secondary beams, as antiprotons of momentum in the range 1.5-15 GeV/c. The storage and cooler rings will allow also to produce radioactive beams of energy in the range 1.5-2 GeV/u, 10000 times more intense than previously available.

Four main collaborations have been formed, addressing issues in different fields of research. The collaboration CBM (Compressed Baryonic Matter) will focus on proton-proton and proton-nuclei collisions, in order to explore a part of the phase diagram of nuclear matter, at larger density and lower temperature compared to high energy experiments as RHIC or ALICE.

The collaboration NUSTAR (Nuclear Structure, Astrophysics and Nuclear Reaction) will study the frontiers of the nuclear stability and the properties of nuclear binding with stable and exotic beams.

APPA is a multi facet collaboration, including several experiments on atomic and plasma physics, biomedicine and materials science. Quantum electrodynamics (QED) can be tested in extreme conditions : very high electromagnetic fields can be created by stripping the electrons from heavy ions, which will result in highly charged ions interacting with antiprotons. The effects of radiation on biological cells is of interest for medicine, radiotherapy and space missions. The interaction of very slow antiprotons with atoms and molecules will be studied. Antiprotons

---

\*e-mail: etomasi@cea.fr

combined with positrons may create anti hydrogen, which can be used to test fundamental symmetries of the forces driving Nature.

We focus here on the hadron physics experiment with antiproton beams, PANDA [2], which will address different aspects of non perturbative QCD. More specifically, the kinematical region accessible at PANDA is interesting for the study of problems related to the understanding of quark confinement, of the origin of the nucleon mass and on the creation of charm and strangeness [3].

## 2 The accelerator complex

Different machines, acceleration cavities and storage rings, are designed in order to optimize the production and the acceleration of several kinds of beams and the existing machine are refurbished or replaced. A scheme of the FAIR complex, the accelerators and the experiment sites is shown in Fig. 1. Technological challenges in accelerator physics are afforded, as for example the ultra-high vacuum ( $10^{-12}$  mbar) which is necessary to keep recirculating the intense ion beams without losses, or diagnostic systems for very intense beams.

The accelerator will consist in high intensity sources of light and heavy ions. A protons ECR source will provide 70 mA proton beam current (35 mA) for multi-turn injection into SIS18. A new proton linear accelerator, *p – linac*, will be built as an injector for high intensity proton beams. The existing UNILAC and ring SIS18 will pre accelerate the ions before injection in the first synchrotron, SIS100 and later on, in a second one, SIS300. Ions will be generated and eventually further converted into secondary beams.

Collector, storage and cooling rings will prepare and optimize the properties of the beams for specific experiments. The time operation of the different rings will be coordinated in such a way that up to four experiments will make use of the beam in the best conditions, simultaneously.

Let us follow the preparation of the antiproton beam. The high intensity proton beam, accelerated by the p-linac at 50 MeV, will be injected in the synchrotrons SIS18/SIS100 and hit the antiproton production target.  $10^7$   $\bar{p}$ /s will be produced at an energy of 3 GeV, injected in the Collector Ring, and then in HESR.

The high quality of the antiproton beams will be insured by two kinds of cooling: electron cooling, and stochastic cooling. In the Collector Ring (CR) secondary ion beams and antiprotons undergo stochastic cooling. Here the mass of some radioactive ions can also be measured. Antiprotons are then accumulated in the Recycled Experimental Storage Ring (RESR) in order to increase their intensity and cooled using electron and stochastic cooling for experiments. In the High-Energy Storage Ring (HESR) the antiproton beams are decelerated to a momentum of 1.7 GeV/c or accelerated up to 14.5 GeV/c.

HESR has, in principle, two modes of operation; high intensity mode (peak luminosity  $2 \times 10^{32}$  cm<sup>-2</sup> s<sup>-1</sup> and momentum spread  $\Delta p/p \approx 10^{-4}$ ) or high resolution mode, which will be available in the first times of operation, which corresponds to ten times reduced peak luminosity and momentum spread  $\Delta p/p \approx 10^{-5}$ .

## 3 The detector

The antiproton beam will hit a pellet target  $4 \times 10^{15}$  cm<sup>-2</sup> thick, surrounded by the PANDA detector (jet or solid targets are also foreseen).

PANDA is therefore a fixed target and an internal target experiment, because the antiprotons which do not interact with the target will recirculate in HESR. The ring and the detector are built and optimized together. It is therefore expected that the performances of this experiment in terms of resolution and luminosity will be significantly higher than what previously achieved.

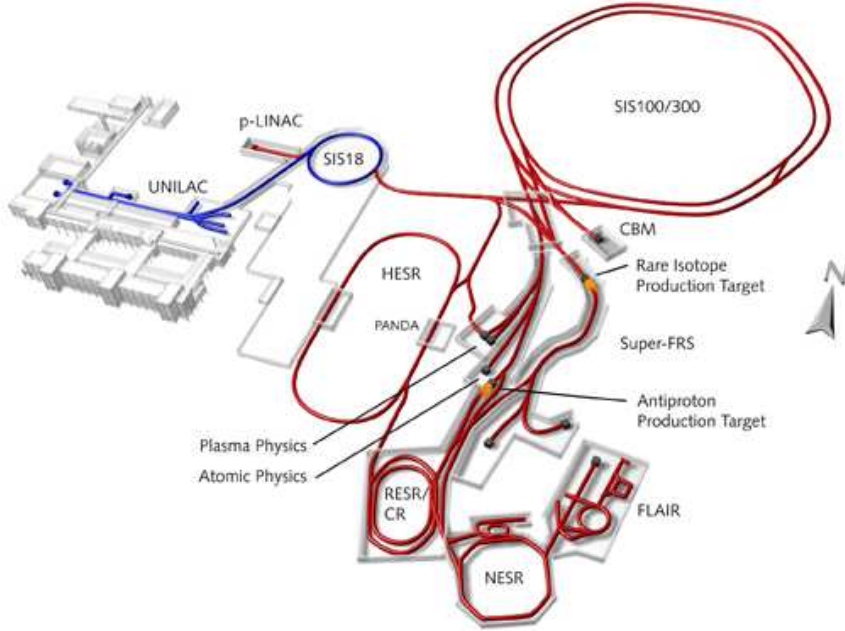


Figure 1: View of the FAIR complex.

The detector is a very compact assembly of several subdetectors with an efficient and flexible design to account for different physics goals, insuring a  $4\pi$  detection with excellent tracking capabilities and momentum resolution.

A schematic view of the PANDA detector is illustrated in Fig. 2. The size of the detector is about 12 m along the beam direction. It is a compact detector, with two magnets, a central 2T solenoid and a forward dipole. Some of the elements are shortly described below. A detailed description can be found in the dedicated technical design reports [2].

The microvertex detector (3 layers of pixel sensors and 2 layers of double sided strips) surrounds the target. The expected resolution is of the order of  $100 \mu\text{m}$  which is mandatory for a good vertex reconstruction for  $D$ ,  $K_S$ , and hyperons.

The central tracker consists of straw tubes (STT) to insure a precise spatial reconstruction of the trajectories of charged particles in a broad momentum range from about a few 100 MeV/c up to 8 GeV/c through the energy loss measurement  $dE/dx$ . The DIRC (Detection of Internally Reflected Cerenkov) will be used for particle identification at polar angles between  $22^\circ$  and  $140^\circ$ , and momentum up to 5 GeV/c. A scintillator tiles detector surrounds the DIRC and will provide PID for slow particles, with a resolution up to 50 ps.

The barrel will be completed by an electromagnetic (EM) calorimeter, consisting of Lead Tungstate  $\text{PbWO}_4$  crystals, to insure an efficient photon detection from 10 MeV to 10 GeV. The geometry is designed to optimize the granularity. The hermiticity of the detection coverage is insured by a forward endcap (3856 crystals) and a backward endcap (600 crystals) in addition to the cylindrical barrel of 11360 crystals. A similar type of crystals has been used by CMS. However, the photon detection in a high luminosity environment and in such a large energy range, is a specific requirement of PANDA compared to previous experiments and demands new solutions for detectors, associated with electronics, and data acquisition. In particular, a low energy threshold of  $\leq 3$  MeV for an individual detector module requires the maximization of the  $\text{PbWO}_4$  light output and the light detection efficiency [4]. An increase of the scintillation light by a factor of four is obtained by cooling the crystals. The PANDA EMC calorimeter will be operated at a temperature of  $T=-25^\circ\text{C}$ . This requires a functional test of all components in a low temperature environment. Moreover, the quality of the crystals themselves has essentially

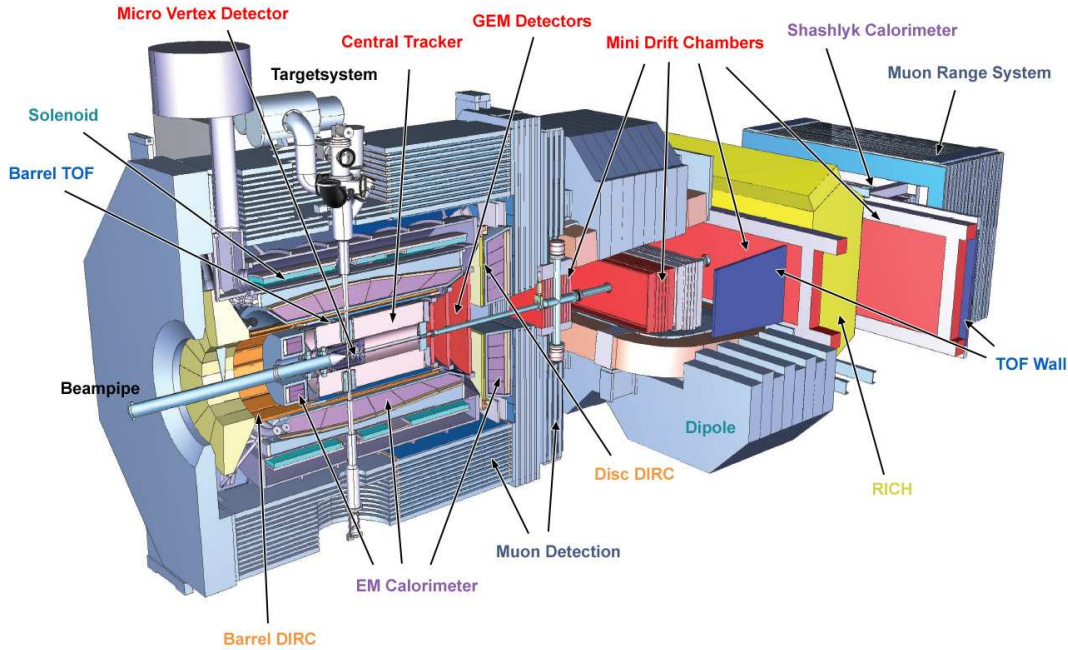


Figure 2: View of the PANDA detector.

improved, by minimizing the impurities. The light produced by each crystal is read out by two rectangular Large Area Avalanche Photodiodes (LAAPD).

Particles emitted at angles smaller than  $22^\circ$  will be detected by three planar stations of Gas Electron Multiplier (GEM) downstream of the target. The GEM foils can sustain high counting rate of particles peaked at forward angles. A hadronic calorimeter for  $K_L$  and neutrons is foreseen in the forward region. Aerogel Ring Imaging Cerenkov Counters located in the endcap of the target spectrometer between polar angles of  $5^\circ$  and  $22^\circ$  will be useful for PID, in particular for  $\pi/K$  separation and information for higher level triggers. The muon identification will be done by Iarocci proportional tubes and with scintillator counters placed outside and inside the solenoid and dipole magnets, in the inner gap of the solenoid yoke and between the hadron calorimeter planes, with a forward angular coverage up to  $60^\circ$ .

In order to collect different types of events no hardware trigger is foreseen, but continuous data acquisition with fast readout followed by an intelligent software trigger is under development.

## 4 The physics

A scheme of the accessible physics objects is shown in Fig. 3. The mass range and the corresponding antiproton momentum are shown respectively on the bottom and top scale. The light meson sector was previously studied with antiproton beams by LEAR and AGS. The vertical line shows the upper limit of LEAR. The kinematical region covered by PANDA is especially well suited for charmonium and open charm spectroscopy. The high resolution will be crucial for the search and the understanding of the properties of gluonic excitations, as glueball and hybrids.

QCD motivated quark potentials, containing a Coulomb-like part and a confinement term, successfully predicted the lower part of the spectrum of Charmonium, the bound  $\bar{c}c$  state. The states are narrow and well separated, therefore they have been well identified by different

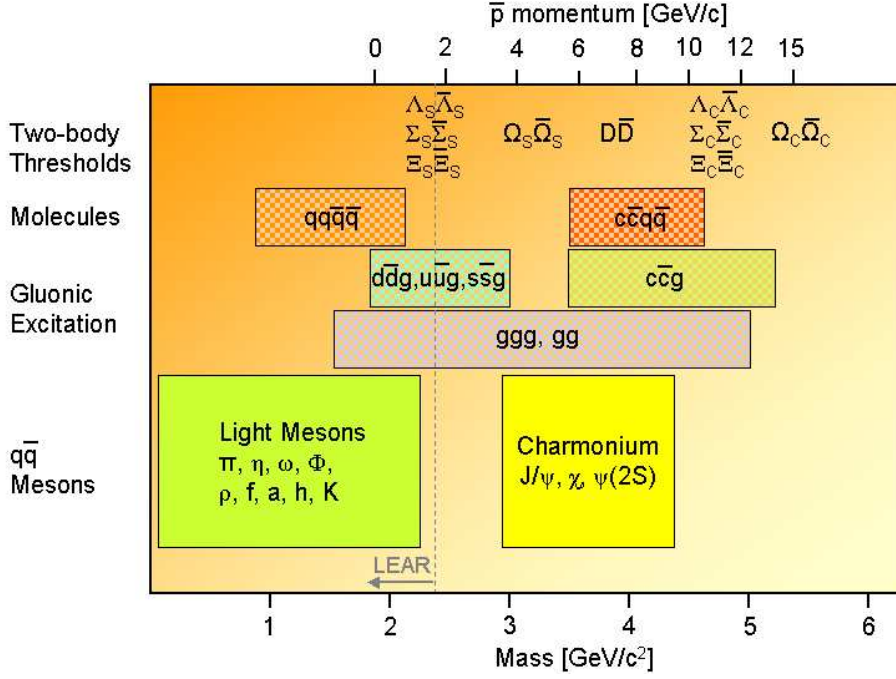


Figure 3: Illustration of the accessible physics. The lower scale shows the mass, the upper scale the corresponding beam momentum where the physical objects (vertical scale) can be observed.

experiments. Still a better knowledge of some masses and widths, as well as the properties of high angular momentum states are desirable. Moreover, since a decade, a large number of charmonium-like states have been observed, not predicted by potential models. They are called X, Y, Z. Their interpretation is still under debate and their quantum numbers mostly unknown. In particular, the states X(3872) and  $Z_c(3900)$  have been seen by the  $e^+e^-$  facilities working in this energy range, BaBar, BES and BELLE. Observed in different decays, still their nature has not been elucidated: excited charmonium,  $D^0\bar{D}^{*0}$  molecule,  $c\bar{c}g$  hybrid, tetraquarks...PANDA is expected to bring original information in this field because of the uniqueness of the antiproton probe at such energy and intensity.

As an example, in Fig. 4 the reconstruction power of the antiprotons is illustrated. The resonance spectrum of  $\chi_{c1}$  is shown as a function of the center of mass energy in  $\bar{p}p$  annihilation through the reaction  $\bar{p}p \rightarrow \chi_{c1} \rightarrow J\psi\gamma \rightarrow e^+e^-\gamma$  (right scale, green circles) [5]. It is compared to the corresponding spectrum measured with Crystal Ball through  $e^+ + e^- \rightarrow \psi' \rightarrow \chi_{c1} \rightarrow J\psi\gamma\gamma \rightarrow e^+e^-\gamma\gamma$  (left scale, red circles). The comparison of the obtained resolution is spectacular: the mass resolution of 10 MeV from  $e^+e^-$ : should be compared with 240 keV obtained with antiprotons at FermiLab: in the experiment E835 the formation rate of a resonance is monitored by the beam parameters, and not driven by the energy resolution of the detectors.

As shown in FermiLab, the resolution which can be achieved with  $\bar{p}$  beams allows a precise energy scan and the profile of a resonance can be well defined. Note that PANDA will show an increase of a factor of five to ten as compared to FERMILab. This is crucial at high energies, where resonances overlap.

PANDA will reach the threshold for charm baryon production, and open the study for open charm associated production: a large sample of  $D\bar{D}$  pairs will be produced, making possible studies of CPT violation in the charm sector. The  $D$  meson formed by a light and a heavy quark plays the role of a "QCD" hydrogen atom. Its production at threshold involves on one hand, a large energy scale, which is necessary to form a  $c$ -quark not pre-existent in the (anti)proton

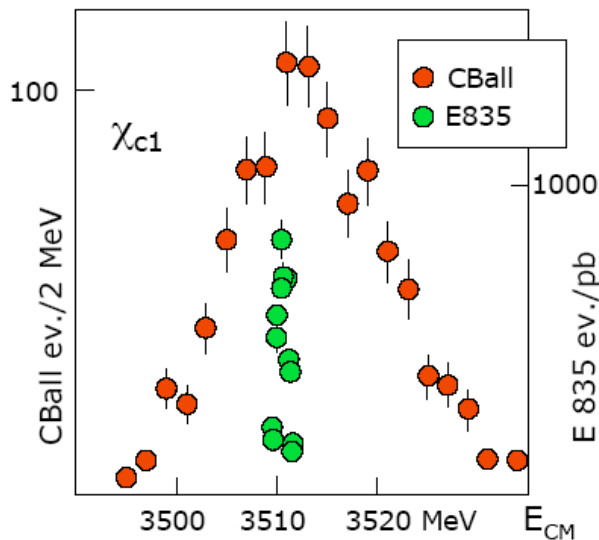


Figure 4: Invariant mass spectrum of  $\chi_{c1}$ , as measured by Crystal Ball (red circles) and E835 (green circles)

valence quarks, and, on the other hand, low kinetic energies, making simpler the spin structure of the reaction matrix.

It is known that antiproton-proton annihilation creates a gluon-rich environment. The interaction between gluons is attractive. It is believed that the difference between the proton mass and the mass of the valence quarks is dynamically created by the interacting gluons. New states can appear, with quantum numbers not allowed by the quark model, called "hybrids" such as flux tube between  $q\bar{q}$  pairs, glueballs (meson-like bound state of gluons). Spectroscopy offers a powerful way to find evidence of gluonic excitations. Most promising is the search for a scalar  $J^{PC} = 0^{++}$  (lightest glueball) through the reaction  $\bar{p}p \rightarrow \pi^0\pi^0\pi^0$ , where the  $\bar{p}p$  system at rest decays into 3 pseudoscalars. The resonance  $0^+$  decays into two pseudoscalars:  $0^+ \rightarrow 0^-0^-$  while the third pseudoscalar removes the excess energy. The Crystal Barrel at LEAR accumulated a large statistics making possible to detect several resonances, visible in the  $3\pi^0$  Dalitz plot, in particular, the  $f_0(1500)$  which could be the lightest good glueball candidate.

A comprehensive review of the topics addressed by PANDA can be found in Ref. [6].

## 5 Time-like electromagnetic proton form factors

Electromagnetic proton form factors (FFs) are fundamental quantities which contain the dynamical information on the internal charge and magnetic distributions of the proton. The electric,  $G_E$  and magnetic,  $G_M$ , FFs can be accessed, in the time-like (TL) region, through a precise measurement of the angular distribution of one of the outgoing leptons in the reaction  $\bar{p} + p \rightarrow e^+ + e^-$ , assuming that the reaction occurs through the exchange of a virtual photon of squared momentum  $q^2$  which decays into a lepton pair. FFs are complex in TL region, and their moduli squared enter in the expression of the differential unpolarized cross section [7]:

$$\frac{d\sigma}{d\cos\theta} = \frac{\pi\alpha^2}{2\beta q^2} \left[ (1 + \cos^2\theta)|G_M|^2 + \frac{1}{\tau} \sin^2\theta|G_E|^2 \right]; \quad \beta = \sqrt{1 - \frac{4M^2}{q^2}}. \quad (1)$$

( $\alpha = e^2/(4\pi) = 1/137$  is the electromagnetic fine constant,  $\beta$  is the beam velocity in the center of mass system, and  $\theta$  is the lepton emission angle. As in the space-like (SL) region accessed

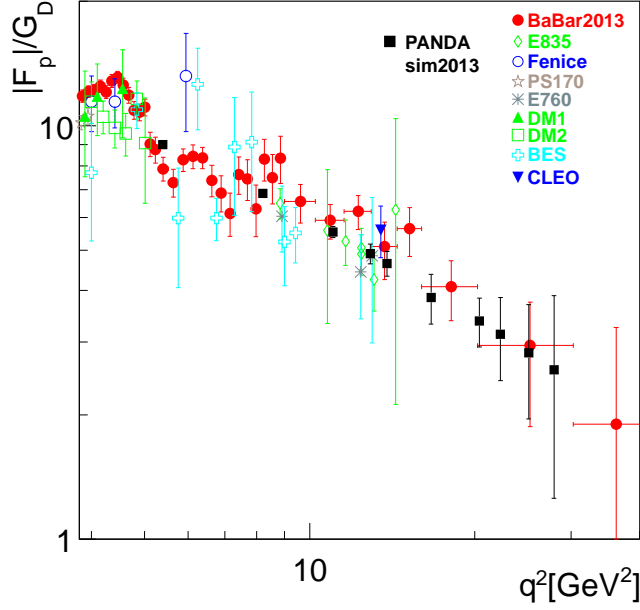


Figure 5:  $q^2$  dependence of the world data on TL FFs. The data from BaBar are shown as red circles. The expectations for PANDA from Ref. [11] are shown as full squares for an integrated luminosity of  $2 \text{ fb}^{-1}$ .

through elastic electron-proton scattering, no interference appears, and the magnetic term is enhanced by the factor  $\tau = q^2/4M^2$ . Unlike in SL region, the differential cross section gives access to the full information on the proton FFs in a single experimental measurement.

The time reverse reaction  $e^+ + e^- \rightarrow \bar{p} + p$  brings the same physical information on the proton internal structure, through the common vertex  $\gamma^* \rightarrow e^+e^-$ . Moreover the process  $e^+ + e^- \rightarrow \bar{p} + p + \gamma$  (initial state radiation) allows to scan a large region of  $q^2$ . When the photon is hard, the cross section of this process can be factorized in a radiator function which depends on the energy and the angle of the hard photon and in the cross section for the process of interest  $e^+ + e^- \rightarrow \bar{p} + p$ .

The individual determination of FFs in TL region has not yet been done due to the limitation in the intensity of antiproton beams or the luminosity of  $e^+e^-$  colliders which did not allow a precise and complete measurement of the angular distribution of the outgoing leptons. The results are often given in terms of an effective FF derived from the total (or integrated) cross section under the assumption  $G_E = G_M = F_p$ :

$$|F_p| = \sqrt{\frac{|G_E|^2 + 2\tau |G_M|^2}{1 + 2\tau}}. \quad (2)$$

At the moment the best data are the ones achieved by BaBar [8, 9], see Fig. 5 where the effective FF is scaled by the dipole function:  $G_D = [1 - q^2/0.71]^{-2}$ . For a recent review the reader is referred to [10]. The data on  $|F_p|$  show several structures, superimposed to a monotone decreasing.

The threshold region is particularly intriguing. Several experiments have been performed, in the near threshold region, with increasing precision. A flat behavior is observed near threshold. At threshold it is expected that only the S-wave plays a role, and  $|G_E^p(4M_p^2)| = |G_M^p(4M_p^2)|$ . Introducing the experimental value of the cross section, one finds  $G(4M_p^2) = 1$ , like in the case of a point-like fermion [12].

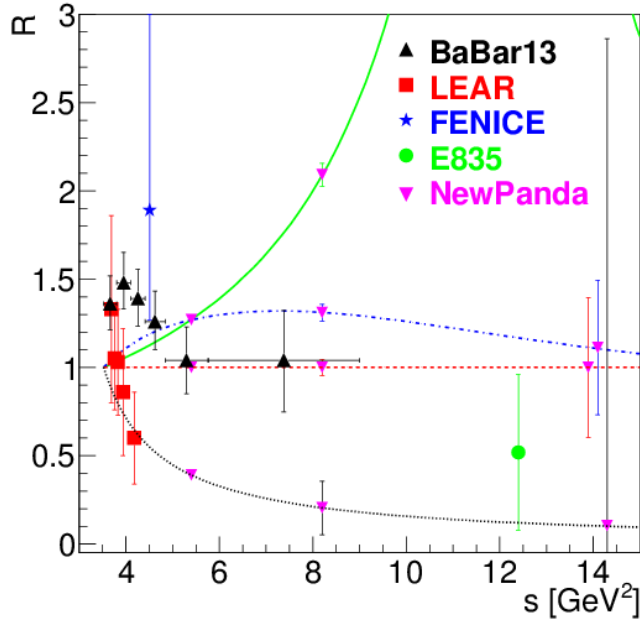


Figure 6: FFs ratio as function of the total energy  $s = q^2$ . Data are from: Ref. [8] (black triangles); Ref. [14] (red squares); Ref. [19] (blue star and green circle). The simulated data for PANDA (magenta triangle down) from [11], have been reported along the prediction of different models for TL ratio: [15, 16] ( $\mathcal{R} = 1$ , dashed line, red), [17] (solid line, green), [18] (dash-dotted line, blue), [20] (dotted line, black).

The important contribution from PANDA will consist also in the fact that the electric and magnetic FFs will be measured separately for the first time, in a wide kinematical range. Note that the models which reproduce qualitatively well the existing data in SL region ( $G_E$  and  $G_M$  for proton and neutron) and  $F_p$  in TL region, may give very different predictions for  $G_E$  and hence for the ratio  $\mathcal{R} = |G_E|/|G_M|$ , as well as for polarization observables in TL region [13]. Attempts of determining  $|G_E|$  and  $|G_M|$  separately, or, more precisely, the ratio  $\mathcal{R}$ , can be found in Ref. [14] (PS170 at LEAR) and more recently in Ref. [8]. The results of the two experiments, although affected by large errors, are not consistent. In the second case a larger value was found, in a wide  $q^2$  range above threshold, and a convergence towards unity at large  $q^2$ .

With the luminosity known at a level of a few percent, PANDA may first determine  $|G_E|$  and  $|G_M|$  separately, for intermediate values of  $q^2$ . The projections for PANDA according to different models are shown in Fig. 6. The statistical error will certainly allow to discriminate among the predictions available today which are reported on the figure.

These data, compared to the corresponding information obtained in electron proton elastic scattering experiments, will constitute a stringent test of the asymptotic behavior predicted by QCD and of analytical properties of the reaction amplitudes. The asymptotic region, where the space-like and time-like values are expected to converge (following analyticity) will be investigated by PANDA.

Moreover, the detection of a pion accompanying the lepton pair,  $\bar{p}p \rightarrow e^+e^-\pi^0$  will allow to access for the first time the "unphysical region" under the  $\bar{p}p$  kinematical threshold, following an idea from Ref. [21], updated in Ref. [22].

The main challenge of these measurements is the identification of the lepton pair in a huge hadronic background, which is larger than the signal by six orders of magnitude, in particular two and three pion emission. Simulations show that this is achievable, keeping an efficiency for

the signal of the order of 50% [11].

## 6 Conclusion

The FAIR facility will represent in next few years the largest European center for nuclear and hadron physics. We have briefly illustrated the FAIR complex, the PANDA detector and described some aspects of the physics program in the fields of charmonium spectroscopy, glueballs, exotics, and nucleon structure.

We overlooked a large part of the foreseen physics program. A review, including also reaction mechanisms, peripheral collisions, in-medium modification of mesons, color transparency, Drell-Yan processes, generalized and transverse parton distributions can be found in the literature [6]. Let us briefly mention here hypernuclear physics. Hypernuclei are obtained replacing one (or more)  $u$  or  $d$  quarks by a  $s$  quark. Very few double hypernuclei have been produced and studied up to now. A specific production method with a dedicated set-up will allow to produce several tens of double hypernuclei/day to be compared to less than 10 (in total) in the past. A unique information on  $\Lambda N$  and  $\Lambda - \Lambda$  interactions which are limited or prevented by the short  $\Lambda$  lifetime in scattering experiments, will be obtained: this represents a unique possibility to study the  $\Lambda - \Lambda$  interaction potential.

Although many discoveries are ongoing at facilities addressing hadron physics issues, in particular  $e^+e^-$  colliders, PANDA has several advantages. In  $e^+e^-$  collisions only states with the photon quantum numbers  $1^{--}$  can be produced, although states with different quantum numbers can be observed in the decay of higher resonances. In  $\bar{p}p$  collisions, all states with quantum numbers allowed by the selection rules can be directly produced. If a resonance appears in the data - generally a resonance is accompanied a light meson- (production mode), a very precise scan of the corresponding energy region can be done by tuning the beam energy exactly at the energy where the resonance was seen. If no counting rate excess appears, this is a clear signature of the exotic nature of the resonance. Moreover, if a resonance appears, the measured width will depend on the beam momentum resolution and not on the detector reconstruction.

The total cross sections for  $\bar{p}p$  annihilation in the PANDA energy domain is of several tens of mb. The cross section for glueballs at PANDA is expected to be several  $\mu\text{b}$  and for hybrids, two orders of magnitude lower. Detailed simulations for several reactions and decay channels [3] show the large potentiality of PANDA. Compared to previous antiproton facilities, PANDA will have a factor of 10 improvement in luminosity and beam momentum resolution as well as a better angular coverage and momentum acceptance.

Presently the PANDA Collaboration is formed by 500 researchers from 63 Institutions in 16 countries. Technical design reports have been published or are in preparation. A recent conference, bringing together the FAIR community and discussing the physics program in the light of the international competition has taken place [23]. The project, which was originally mainly European, is now attracting worldwide collaborators.

## References

- [1] The new large scale accelerator facility in Europe website, URL: <http://www.fair-center.eu>  
<http://www.gsi.de/FAIR>.
- [2] <http://www.gsi.de/PANDA>.
- [3] [PANDA Collaboration], Physics Performance Report for PANDA: Strong Interaction Studies with Antiprotons, arXiv:0903.3905 [hep-ex];
- [4] M. Kavatsyuk *et al.* [PANDA Collaboration], Nucl. Instrum. Meth. A **648** (2011) 77.

- [5] M. Andreotti, S. Bagnasco, W. Baldini, D. Bettoni, G. Borreani, A. Buzzo, R. Calabrese and R. Cester *et al.*, Nucl. Phys. B **717**, 34 (2005).
- [6] U. Wiedner, Prog. Part. Nucl. Phys. **66** (2011) 477.
- [7] A. Zichichi, S. Berman, N. Cabibbo, R. Gatto, Nuovo Cim. **24**, 170 (1962).
- [8] J. Lees, *et al.*, Phys. Rev. D **87**, 092005 (2013).
- [9] J. P. Lees *et al.* [BaBar Collaboration], Phys. Rev. D **88**, 072009 (2013).
- [10] S. Pacetti, R. Baldini-Ferroli and E. Tomasi-Gustafsson (2014), DOI: 10.1016/j.physrep.2014.09.005.
- [11] A. Dbeyssi, Ph.D. thesis, Université Paris-sud (2013).
- [12] R. Baldini, S. Pacetti, A. Zallo, A. Zichichi, Eur. Phys. J. A **39**, 315 (2009).
- [13] E. Tomasi-Gustafsson, F. Lacroix, C. Duterte, G. Gakh, Eur. Phys. J. A **24**, 419 (2005).
- [14] G. Bardin, *et al.*, Nucl. Phys. B **411**, 3 (1994).  
@articleBaldini:2005xx R. Baldini, *et al.*, Eur. Phys. J. **C46** (2006) 421428.
- [15] V. Matveev, R. Muradyan, A. Tavkhelidze, Teor. Mat. Fiz. **15**, 332 (1973).
- [16] S. J. Brodsky, G. R. Farrar, Phys. Rev. Lett. **31**, 1153 (1973).
- [17] F. Iachello, Q. Wan, Phys. Rev. C **69**, 055204 (2004).
- [18] E. L. Lomon, S. Pacetti, Phys. Rev. D **85**, 113004 (2012).
- [19] R. Baldini, C. Bini, P. Gauzzi, M. Mirazita, M. Negrini and S. Pacetti, Eur. Phys. J. C **46**, 421 (2006).
- [20] E. Kuraev, E. Tomasi-Gustafsson, A. Dbeyssi, Phys. Lett. B **712**, 240 (2012).
- [21] M. P. Rekalov, Sov. J. Nucl. Phys. **1**, 760 (1965).
- [22] E. A. Kuraev, Y. M. Bystritskiy, V. V. Bytev, E. Tomasi-Gustafsson, A. Dbeyssi and E. Tomasi-Gustafsson, J. Exp. Theor. Phys. **115**, 93 (2012).
- [23] <http://indico.gsi.de/conferenceDisplay.py?confId=2443>.